

DEUTSCHES ELEKTRONEN-SYNCHROTRON DESY

DESY 84-043
December 1984



PRODUCTION AND DECAY OF THE F-MESON IN e^+e^- ANNIHILATION

AT 10 GeV CENTRE-OF-MASS ENERGY.

by

ARGUS Collaboration

ISSN 0418-9833

NOTKESTRASSE 85 · 2 HAMBURG 52

DESY behält sich alle Rechte für den Fall der Schutzrechtserteilung und für die wirtschaftliche Verwertung der in diesem Bericht enthaltenen Informationen vor.

DESY reserves all rights for commercial use of information included in this report, especially in case of filing application for or grant of patents.

To be sure that your preprints are promptly included in the
HIGH ENERGY PHYSICS INDEX ,
send them to the following address (if possible by air mail) :



DESY
Bibliothek
Notkestrasse 85
2 Hamburg 52
Germany

**PRODUCTION AND DECAY OF THE F MESON
IN e^+e^- ANNIHILATION AT 10 GeV CENTRE-OF-MASS ENERGY.**

THE ARGUS COLLABORATION.

H. ALBRECHT, U. BINDER, G. DREWS, G. HARDER, H. HASEMANN,
A. PHILIPP, W. SCHMIDT-PARZEFALL, H. SCHRÖDER,
H. D. SCHULZ, F. SELONKE, R. WURTH.
DESY, HAMBURG, GERMANY.

A. DRESCHER, B. GRÄWE, W. HOFMANN¹, A. MARKEES²,
U. MATTHIESSEN, H. SCHECK, J. SPENGLER, D. WEGENER.
INSTITUT FÜR PHYSIK, UNIVERSITÄT DORTMUND³, GERMANY.

R. HELLER⁴, K. R. SCHUBERT, J. STIEWE, R. WALDI, S. WESELER.
INSTITUT FÜR HOCHENERGIEPHYSIK,
UNIVERSITÄT HEIDELBERG⁵, GERMANY.

N. N. BROWN⁶, K. W. EDWARDS⁶, W. R. FRISKEN⁷, CH. FUKUNAGA⁷,
D. J. GLEKINSON⁸, D. M. GINGRICH⁸, M. GODDARD⁷,
P. C. H. KIM⁸, R. KUTSCHKE⁸, D. B. MACFARLANE⁸,
J. A. MCKENNA⁸, K. W. MCLEAN⁶, A. W. NILSSON⁶, R. S. ORR⁸,
P. PADLEY⁸, P. M. PATEL⁸, J. D. PRENTICE⁸,
H. G. J. SEYWERD⁸, B. J. STACEY⁸, T. S. YOON⁸, J. C. YUN⁶,
INSTITUTE OF PARTICLE PHYSICS⁹, CANADA.

R. AMMAR, D. COPPAGE, R. DAVIS, S. KANEKAL, N. KWAK.
UNIVERSITY OF KANSAS¹⁰, LAWRENCE, KANSAS, USA.

P. BÖCKMANN¹¹, L. JÖNSSON, Y. OKU.
INSTITUTE OF PHYSICS, UNIVERSITY OF LUND¹², SWEDEN.

M. DANILOV, V. LUBIMOV, V. MATVEEV, N. NAGOVITSIN,
V. RYTSOV, A. SEMENOV, YU. SEMENOV, V. SHEVCHENKO,
V. SOLOSHENKO, V. SOFOV, I. TICHOMIROV, YU. ZAITSEV.
INSTITUTE OF THEORETICAL AND EXPERIMENTAL PHYSICS,
MOSCOW, USSR.

R. CHILDERS, C. W. DARDEN, AND H. GENNOW¹³.
UNIVERSITY OF SOUTH CAROLINA¹⁴, COLUMBIA, S. C., USA.

¹Now at UC, Berkeley, USA

²Now at Swiss Administration, Berne, Switzerland

³Supported by the Bundesministerium für Forschung und Technologie, Federal Republic of Germany.

⁴Now at DESY.

⁵McGill University, Montreal.

⁶Carleton University, Ottawa.

⁷York University, Downsview.

⁸University of Toronto, Toronto.

⁹Supported by the Natural Sciences and Engineering Research Council, Canada.

¹⁰Supported by the U.S. National Science Foundation and a University of Kansas Faculty Improvement award.

¹¹Now at CERN.

¹²Supported by the Swedish Research Council.

¹³On leave from the University of Stockholm, Sweden.

¹⁴Supported by the U.S. Department of Energy, under contract DE-AS09-80ER10690.

Using the ARGUS detector at DORIS, we have observed the production of F^\pm mesons in e^+e^- annihilation at a centre of mass energy of 10 GeV through their subsequent decays into $\phi\pi^\pm$ and $\phi\pi^+\pi^-\pi^\pm$. The values obtained for $[R(e^+e^- \rightarrow F X) \cdot \text{Branching Ratio}]$ are $(1.47 \pm 0.32 \pm 0.20)\%$ and $(1.63 \pm 0.42 \pm 0.41)\%$ respectively. The observed mass is $(1973.6 \pm 2.6 \pm 3.0) \text{ MeV}/c^2$. The F momentum spectrum is as expected for the fragmentation of c quarks into charmed mesons, but is somewhat softer than for fragmentation into D^* mesons. The relevant angular distributions are consistent with a spin zero assignment of the F meson.

We report here evidence for the production of F^\pm mesons in e^+e^- annihilation at $\sqrt{s} = 10$ GeV, and their decay into two channels. The data provide information both on the fragmentation of c quarks into $c\bar{F}$ states and on F decay branching ratios. Since understanding of heavy quark hadronisation is limited, it is interesting to compare the F fragmentation function with those already measured in D and D^* production. Measurement of the branching ratios of weak F decays gives insight into the interplay of the various possible decay mechanisms. Although the spectator model for heavy quark decay ⁽¹⁾ describes the broad features of these decays, its shortcomings have already been demonstrated by results on the D^0 , D^{\pm} lifetimes and also by the observation of F decay final states containing neither an s nor an \bar{s} quark ^(2,3). Studies of F production and decay will contribute considerably to the resolution of these questions.

Early experimental searches ^(2,4) for the F meson showed an enhancement of mass 2020 MeV/ c^2 in channels containing η, η' , and ϕ , all of which are expected in the quark decay (spectator) model. In 1983, CLEO ⁽⁵⁾ reported a state at 1970 MeV/ c^2 decaying to $\phi\pi$, and presented strong evidence that it is indeed the F meson. Two subsequent experiments ⁽⁶⁾ have corroborated this discovery. The ARGUS collaboration has reported ⁽⁷⁾ the observation of the spin 1 excited state of the F , the F^* , which decays into $F\gamma$, where the F is seen in the $\phi\pi$ channel. We now report a detailed study of F production and decay both in the $\phi\pi$ channel and, for the first time, in the $\phi\pi^+\pi^-\pi^\pm$ channel.

The data presented here were collected using the ARGUS spectrometer at the DORIS II e^+e^- storage ring at DESY. The centre of mass energy range was from 9.4 to 10.6 GeV/ c^2 . A short description of the detector and its trigger may be found in reference 8, and its particle identification capabilities are described in reference 9. Data from a 62.7 pb $^{-1}$ sample, comprising 8.6 pb $^{-1}$ on the $\Upsilon(9460)$ resonance, 38.2 pb $^{-1}$ on the $\Upsilon(10023)$, 11.1 pb $^{-1}$ on the $\Upsilon(10573)$, and 4.8 pb $^{-1}$ on the continuum, were used for this analysis.

Events corresponding to e^+e^- annihilation into a multihadron final state were selected, as in reference 8, by requiring ≥ 4 tracks reconstructed in the drift chamber and associated with the primary interaction point. Only tracks having $|\cos\theta| \leq 0.9$ and $p_T \geq 60$ MeV/ c have been used in order to give a well defined acceptance and well measured tracks. In searching for the F signal, particle identification is essential. We have used both the specific ionisation measurements in the drift chamber (dE/dx) and time-of-flight (ToF) information for particle identification. A more detailed description is given in reference 9. Briefly, for each

track in an event, the probability for each mass hypothesis is:

$$P_i = \frac{f_i e^{-\chi_i^2/2}}{\sum_j f_j e^{-\chi_j^2/2}}, \quad i, j = \pi, K, p \quad f_\pi = 5, \quad f_K, f_p = 1, \quad (1)$$

where the f_i 's are relative production abundances. In forming effective mass combinations, a track was used for all mass hypotheses for which this particle identification probability was greater than 5%. Almost all tracks with momenta below 700 MeV/ c are uniquely identified. As the momentum increases beyond 700 MeV/ c , the proportion of ambiguous tracks increases steadily.

The invariant mass distribution of all K^+K^- pairs is shown in figure 1. A clear ϕ signal is evident. A fitted Breit-Wigner resonance plus 3rd order polynomial background gives a mass of $(1019.7 \pm 1 \pm 1.1)$ MeV/ c^2 , a full width of (8.1 ± 0.4) MeV/ c^2 and (5079 ± 276) events above background within ± 15 MeV/ c^2 of the ϕ mass. The mass and width (including detector resolution) are in good agreement with the accepted values ⁽¹⁰⁾.

To search for the decay modes $F^\pm \rightarrow \phi\pi^\pm$ and $F^\pm \rightarrow \phi\pi^+\pi^-\pi^\pm$, all combinations of K^+K^- candidates with invariant mass within ± 15 MeV/ c^2 of the ϕ mass, and with $\chi^2 \leq 16$ for the mass hypothesis, were taken as ϕ candidates. Each ϕ was then combined with all π^\pm and $(3\pi)^\pm$ candidates in the event. The following Monte Carlo motivated cuts were also applied:

$$p_{\phi\pi} \geq 1.5 \text{ GeV}/c, \quad -1.0 \leq \cos\theta_\phi \leq 0.8$$

for all $\phi\pi$ combinations

$$p_{\phi 3\pi} \geq 2.2 \text{ GeV}/c$$

for all $\phi 3\pi$ combinations

where θ_ϕ is the angle, with respect to the F boost direction, of the ϕ in the F 's rest frame.

The resulting invariant mass distributions for the $\phi\pi$ and $\phi 3\pi$ are shown in figures 2a and 2b, respectively. Both distributions show enhancements near 1970 MeV/ c^2 . A gaussian of fixed width plus a 3rd order polynomial background was fitted to each distribution. Table 1 shows the resulting numbers of fitted events. Combining the two channels as independent observations, the total statistical significance of the signal is 6.2 standard deviations.

The values of the fixed widths used for these fits were obtained from Monte Carlo studies: $\sigma = 16.8 \text{ MeV}/c^2$ for $\phi\pi$, and $\sigma = 11.2 \text{ MeV}/c^2$ for the $\phi 3\pi$ channel. In the ARGUS Monte Carlo, events are generated for the process $e^+e^- \rightarrow c\bar{c}$ and then fragmented according to the Field and Feynman model (11). The resulting particles are tracked through a simulation of the ARGUS detector and events are then reconstructed and analysed with the standard programs.

The fitted masses in the two channels are consistent. The mean mass is $(1973.6 \pm 2.6 \pm 3.0) \text{ MeV}/c^2$, weighting by the inverse square of the error on mass in each channel. The systematic error is primarily due to the uncertainty in the magnetic field calibration. The mass agrees well with previously reported results in the $\phi\pi$ channel (5,6).

No signal is seen above background in the $KK\pi$ ($KK3\pi$) mass distribution when the analysis is repeated with K^+K^- invariant mass in a $52 \text{ MeV}/c^2$ ($30 \text{ MeV}/c^2$) sideband outside the ϕ mass band, as shown in Figures 3a and 3b. In searching for a signal in the sideband distributions, we fitted gaussians of width equal to the Monte Carlo predictions and mass equal to that found for the signals within the ϕ band. The fitted numbers of events for the sideband ϕ signals are shown in Table 1.

In addition, we have checked that the angular distributions of $F \rightarrow \phi\pi$ and $F \rightarrow \phi 3\pi$ are consistent with the $J^P = 0^-$ assignment of the F meson.

The angular distribution of the ϕ (with respect to the F boost direction) in the F 's rest frame is isotropic, as expected, since the F has spin zero. The angular distribution was obtained by dividing the invariant mass distribution of each channel into five bins of $\cos\theta_\phi$, and extracting the F signal in each bin. Acceptance corrections were then applied, the results were normalized, and both channels were combined using weighted means. The resulting distribution is shown (solid points) along with the background distribution (open squares), and the expected isotropic distribution (solid line), in Figure 4a.

In the $F \rightarrow \phi\pi$ decay, the angular distribution of the K^+ in the ϕ 's rest frame (with respect to the π) should be of the form $\cos^2\theta_K$, since the ϕ must have zero helicity in the F 's rest frame. The signal was extracted as in the ϕ angular distribution, acceptance corrected and normalized, and is shown in Figure 4b (solid points) along with the background distribution (open squares), and the expected $\cos^2\theta_K$ distribution (solid curve).

The background angular distributions were obtained by taking the number of entries un-

der the peak in each angular bin in a region $72 \text{ MeV}/c^2$ wide for the $\phi\pi$, and $56 \text{ MeV}/c^2$ wide for the $\phi 3\pi$. The acceptance corrections were then applied, and the resulting distributions were normalized. The angular distributions of the background differ from those of the signal.

It is expected (12) that a charmed meson resulting from c quark fragmentation will have a hard momentum spectrum. We have measured the momentum spectrum of the F by dividing the invariant mass distributions into five bins of x_p , where

$$x_p = \frac{PF}{P_{\text{max}}}, \quad P_{\text{max}} = \sqrt{E_{\text{beam}}^2 - M_F^2}, \quad (2)$$

and extracting the F signal in each bin. The results in the two channels were corrected for the momentum dependent acceptance and combined using weighted means to give the final result in Figure 4c. The x_p distribution is hard and conforms to the expectation for heavy quark production. Peterson et al. (13) suggest a fragmentation function of the form:

$$\frac{dN}{dx_p} \sim \frac{1}{x_p \left(1 - \frac{1}{x_p} - \frac{\epsilon}{1-x_p}\right)^2} \quad (3)$$

while Kartvelishvili et al. (14) propose:

$$\frac{dN}{dx_p} \sim x_p^\alpha (1-x_p) \quad (4)$$

Fitting these forms to the measured distribution yields $\epsilon = .50_{-0.14}^{+0.22}$ with $\chi^2 = 2.9$ for 3 degrees of freedom (solid curve) and $\alpha = .64_{-0.20}^{+0.23}$ with $\chi^2 = 2.3$ for 3 degrees of freedom (dashed curve), respectively, shown in Figure 4c. The F fragmentation function measured here is softer than that of the D^* (9). This softening is partly explained by the ratio of the masses of the s and u or d quarks accompanying the c quark in the F and D^* mesons respectively. Some slight softening of the fragmentation function is a consequence of the fact that a large proportion of the observed F 's are due to the cascade decay, $F^* \rightarrow F \gamma$ (7).

The F production cross section times the branching ratio for each channel ($\sigma_F \cdot BR$), and the production cross section times branching ratio relative to μ pair production ($R_F \cdot BR$) are shown in Table 1. These values are acceptance corrected and extrapolated to cover the entire x_p range using equation (3) with the fitted value of $\epsilon = .50$. The systematic error in the $\phi 3\pi$ channel is increased due to the uncertainty in the F width in this channel. If the signals are fitted with free widths, the $\phi\pi$ width is consistent with Monte Carlo studies, but the $\phi 3\pi$ width is larger than the Monte Carlo width and has a large uncertainty. Our value for ($R_F \cdot BR$) in the $\phi\pi$ channel is in good agreement with the CLEO result (6) $(2.0 \pm 0.5)\%$,

obtained at the same e^+e^- energy, but it is somewhat smaller than the TASSO result ⁽⁶⁾ ($6.4 \pm 1.3 \pm 1.9$)%, obtained at a higher energy.

The ratio

$$\frac{\text{BR}(F^\pm \rightarrow \phi\pi^+\pi^-\pi^\pm)}{\text{BR}(F^\pm \rightarrow \phi\pi^\pm)} = 1.11 \pm 0.37 \pm 0.28 \quad (5)$$

is smaller than the ratio for the analogous D^0 decays: ⁽⁹⁾

$$\frac{\text{BR}(D^0 \rightarrow K^-\pi^+\pi^+\pi^-)}{\text{BR}(D^0 \rightarrow K^-\pi^+)} = 2.17 \pm 0.35 \quad (6)$$

A smaller ratio is expected for the F decays due to phase space considerations.

To conclude, we have observed the decay $F^\pm \rightarrow \phi\pi^+\pi^-\pi^\pm$ and confirmed the observation of $F^\pm \rightarrow \phi\pi^\pm$. The average mass of the F is found to be $(1973.6 \pm 2.6 \pm 3.0)$ MeV/c². The branching ratio of $F^\pm \rightarrow \phi(3\pi)^\pm$ is $(1.11 \pm .37 \pm .28)$ times that of $F^\pm \rightarrow \phi\pi^\pm$. The angular distributions of the ϕ (in both channels) and the K^+ (in the $\phi\pi$ channel) are consistent with a spin zero assignment of the F. Finally, the fragmentation function of the F is found to be of the general form expected for heavy quark fragmentation.

TABLE I

FITTED RESULTS FOR F^\pm DECAY CHANNELS		
	$\phi\pi^\pm$	$\phi\pi^+\pi^-\pi^\pm$
Uncorrected # of Events	$100.1^{+22.1}_{-21.4}$	$62.4^{+16.2}_{-10.3}$
Significance (σ)	4.7	4.0
Mass (MeV/c ²)	$1972.8 \pm 3.1 \pm 3.0$	$1975.7 \pm 4.7 \pm 3.0$
Total Acceptance ¹ (%)	12.8	7.2
$\sigma_F \cdot \text{BR}$ (pb)	$12.7 \pm 2.8 \pm 1.7$	$14.1 \pm 3.6 \pm 3.5$
$R_F \cdot \text{BR}$ (%)	$1.47 \pm 0.32 \pm 0.20$	$1.63 \pm 0.42 \pm 0.41$
Sideband ϕ Control Sample		
Uncorrected # of Events	16.9 ± 19.5	-1.8 ± 13.7

σ_F = inclusive cross section for $e^+e^- \rightarrow F^\pm X$

BR = Branching Ratio of F decay mode

$$R_F = \frac{\sigma_F}{\sigma(e^+e^- \rightarrow \mu^+\mu^-)}$$

¹ A factor of .49 has been included for the unseen ϕ decay channels.

ACKNOWLEDGEMENTS

It is a pleasure to thank E. Michel, W. Reinsch, H. Heller, Mrs. E. Konrad and Mrs. U. Djuanda for their competent technical help in running the experiment and processing the data. We thank Drs. H. Neemann, K. Wille and the DORIS group for the good operation of the storage ring. The visiting groups wish to thank the DESY directorate for the support and kind hospitality extended to them.

FIGURE CAPTIONS

Fig. 1 K^+K^- invariant mass distribution in $e^+e^- \rightarrow K^+K^-X$.

Fig. 2a $K^+K^-\pi^\pm$ invariant mass distribution with $\text{mass}(K^+K^-)$ in the ϕ region, with cuts on $p_{KK\pi} \geq 1.5 \text{ GeV}/c$ and $-1.0 \leq \cos\theta_\phi \leq 0.8$.

Fig. 2b $K^+K^-\pi^+\pi^-\pi^\pm$ invariant mass distribution with $\text{mass}(K^+K^-)$ in the ϕ region, and $p_{KK\pi} \geq 2.2 \text{ GeV}/c$.

Fig. 3a $K^+K^-\pi^\pm$ invariant mass distribution with $\text{mass}(K^+K^-)$ outside the ϕ region with cuts $p_{KK\pi} \geq 1.5 \text{ GeV}/c$ and $-1.0 \leq \cos\theta_\phi \leq 0.8$.

Fig. 3b $K^+K^-\pi^+\pi^-\pi^\pm$ invariant mass distribution with $\text{mass}(K^+K^-)$ outside the ϕ region and with a cut on $p_{KK\pi} \geq 2.2 \text{ GeV}/c$.

Fig. 4a Acceptance corrected angular distribution of the ϕ in the F rest frame (with respect to the F boost direction) for the combined $\phi\pi$ and $\phi 3\pi$ channels (solid points). The corresponding background distribution is also shown (open squares). The solid line is the expected isotropic distribution.

Fig. 4b Acceptance corrected angular distribution of the K^+ in the ϕ rest frame (with respect to the π direction) for the $\phi\pi$ (solid points). The corresponding background distribution is also shown (open squares). The solid curve is the expected $\cos^2\theta_K$ distribution.

Fig. 4c Acceptance corrected fragmentation function of the F meson in $e^+e^- \rightarrow FX$ for the two channels $F \rightarrow \phi\pi$ and $F \rightarrow \phi 3\pi$ combined, where $x_p = p_F/p_{\text{max}}$. The solid curve is a fit to the function of Peterson et al. (15), the dashed curve is a fit to that of Kartvelishvili et al. (14).

REFERENCES

1. B.W.Lee, M.K.Gaillard and J.Rosner, *Rev. Mod. Phys.*, **47** (1975), 277.
D.Fakirov and B.Stech, *Nucl. Phys.*, **B133** (1978), 315.
2. R.Ammar et al., *Phys. Lett.*, **94B** (1980), 118.
N.Ushida et al., *Phys. Rev. Lett.*, **51** (1983), 2362 and **48** (1982), 844.
3. W.Bernreuther, B.Stech and O.Nachtmann, *Z. Physik*, **C4** (1980), 257.
H.Fritsch and P.Minkowski, *Phys. Lett.*, **90B** (1980), 455.
4. R.Brandelik et al. (DASP), *Phys. Lett.*, **80B** (1979), 412.
D.Aston et al. (OMEGA), *Phys. Lett.*, **100B** (1981), 91.
D.Aston et al. (OMEGA), *Nucl. Phys.*, **B189** (1981), 205.
M.Atkinson et al. (OMEGA), *Z. Physik*, **C17** (1983), 1.
M.Aquilar-Benitez et al. (EHS), *Phys. Lett.*, **122B** (1983), 312.
5. A.Chen et al. (CLEO), *Phys. Rev. Lett.*, **51** (1983), 634.
6. M.Althoff et al. (TASSO), *Phys. Lett.*, **136B** (1984), 130.
R.Bailey et al. (ACCMOR), *Phys. Lett.*, **139B** (1984), 320.
7. H.Albrecht et al. (ARGUS), *Phys. Lett.*, **146B** (1984), 111.
8. H.Albrecht et al. (ARGUS), *Phys. Lett.*, **134B** (1984), 137.
9. H.Albrecht et al. (ARGUS), DESY 84-073, to be published in *Phys. Lett. B*
10. Particle Data Group, *Rev. Mod. Phys.* **56** (1984), vol.2, Part II, S1.
11. R.D.Field and R.P.Feynman, *Nucl. Phys.*, **B136** (1978), 1.
12. J.D.Bjorken, *Phys. Rev.*, **D17** (1978), 171.
M.Suzuki, *Phys. Lett.*, **71B** (1977), 139.
13. C.Peterson et al., *Phys. Rev.*, **D21** (1983), 105.
14. V.G.Kartvelishvili et al., *Yad. Fiz.*, **38** (1983), 1563 as translated in
Sov. J. Nucl. Phys., **38** (1983), 952.

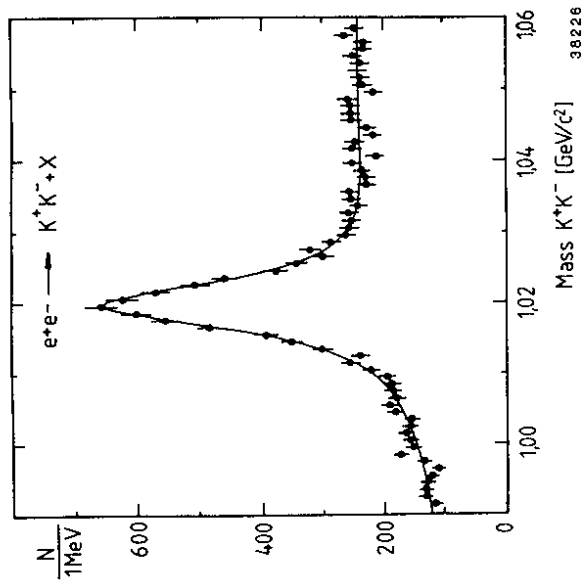


Fig. 1 K^+K^- invariant mass distribution in $e^+e^- \rightarrow K^+K^- X$.

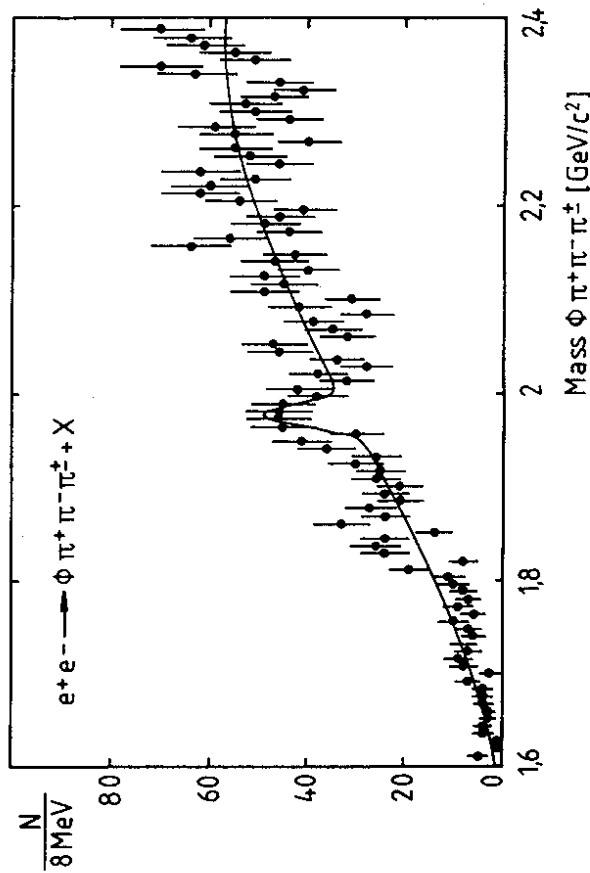
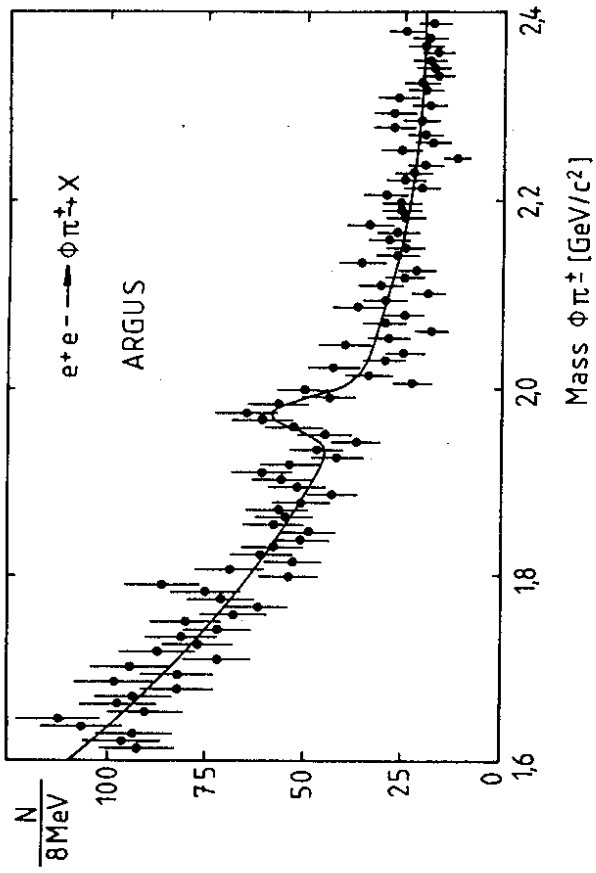


Fig. 2a $K^+K^-\pi^+\pi^-$ invariant mass distribution with $\text{mass}(K^+K^-)$ in the ϕ region, with cuts on $p_{K^+K^-} \geq 1.5 \text{ GeV}/c$ and $-1.0 \leq \cos\theta_\phi \leq 0.8$.

Fig. 2b $K^+K^-\pi^+\pi^-$ invariant mass distribution with $\text{mass}(K^+K^-)$ in the ϕ region, and $p_{K^+K^-} \geq 2.2 \text{ GeV}/c$.

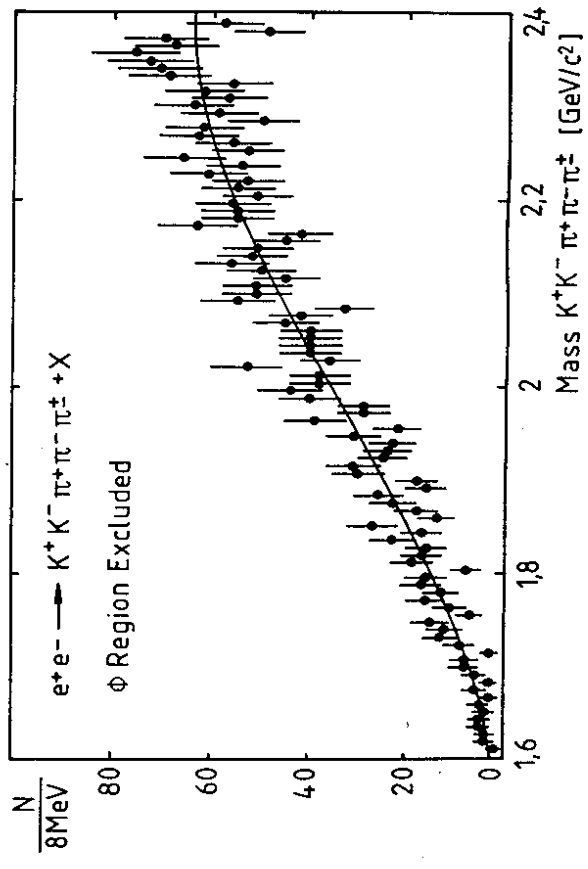
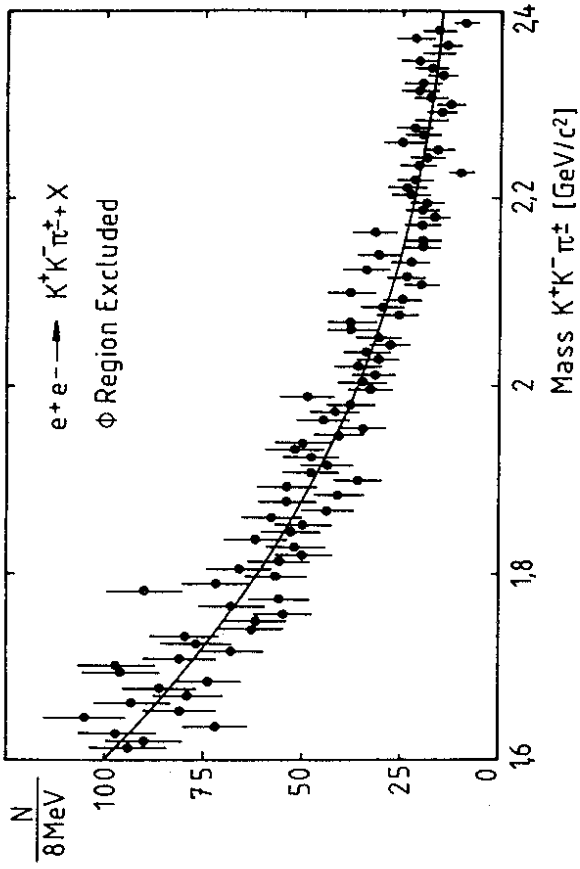


Fig. 3a $K^+K^-\pi^+\pi^-$ invariant mass distribution with $\text{mass}(K^+K^-)$ outside the ϕ region with cuts $p_{K^+K^-} \geq 1.5 \text{ GeV}/c$ and $-1.0 \leq \cos\theta_\phi \leq 0.8$.

Fig. 3b $K^+K^-\pi^+\pi^-$ invariant mass distribution with $\text{mass}(K^+K^-)$ outside the ϕ region and with a cut on $p_{K^+K^-} \geq 2.2 \text{ GeV}/c$.

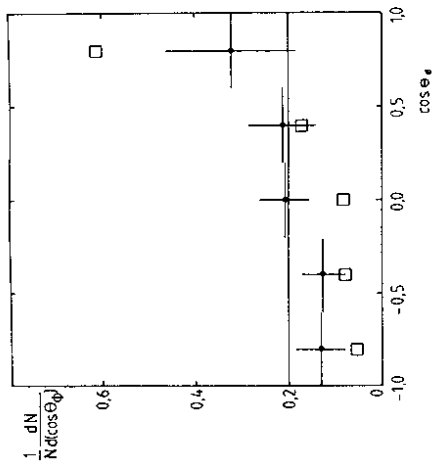


Fig. 4a Acceptance corrected angular distribution of the ϕ in the F rest frame (with respect to the F boost direction) for the combined $\phi\pi$ and $\phi 3\pi$ channels (solid points). The corresponding background distribution is also shown (open squares). The solid line is the expected isotropic distribution.

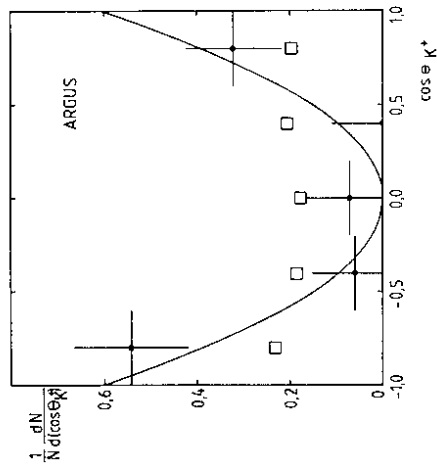


Fig. 4b Acceptance corrected angular distribution of the K^+ in the ϕ rest frame (with respect to the π direction) for the $\phi\pi$ (solid points). The corresponding background distribution is also shown (open squares). The solid curve is the expected $\cos^2 \theta_K$ distribution.

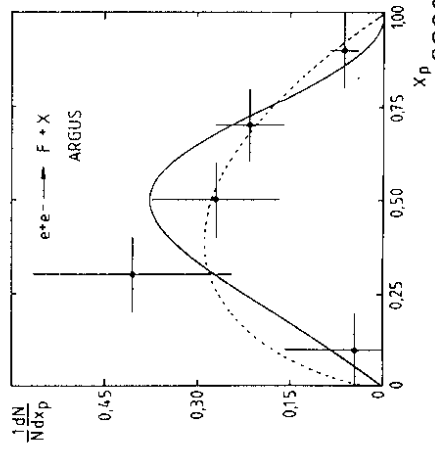


Fig. 4c Acceptance corrected fragmentation function of the F meson in $e^+e^- \rightarrow F X$ for the two channels $F \rightarrow \phi\pi$ and $F \rightarrow \phi 3\pi$ combined, where $x_p = p_F/p_{max}$. The solid curve is a fit to the function of Peterson et al. (13), the dashed curve is a fit to that of Kartvelishvili et al. (14).